Pseudo-Casimir effect in nematic liquid crystals in frustrating geometries

P. Ziherl,[1,2,*] F. Karimi Pour Haddadan,[2] R. Podgornik,[1,2] and S. Žumer[1,2]

[1]*J. Stefan Institute, Jamova 39, SI-1000 Ljubljana, Slovenia*
[2]*Department of Physics, University of Ljubljana, Jadranska 19, SI-1000 Ljubljana, Slovenia*

We study theoretically the fluctuation-induced structural force in nematic systems frustrated by external fields. We focus on the uniform director structure in the hybrid-aligned film characterized by opposing surface fields and in the Fréedericksz cell where frustration arises from competing bulk and surface fields. We find that frustration gives rise to several interesting features of the interaction, including a crossover from attraction at small distances to repulsion at large distances. The fluctuation-induced interaction is enhanced substantially by frustration, the enhancement being progressively stronger on approaching the transition from uniform to distorted structure. At the structural transition the interaction diverges and we show that the pretransitional singularity is universal.

PACS number(s): 61.30.Cz, 61.30.Gd

I. INTRODUCTION

Just as quantum fluctuations of the electromagnetic field within an evacuated conducting container induce an attractive force between its walls—which is referred to as the Casimir effect [1–3]—thermal fluctuations of order in a correlated fluid mediate an interaction between objects immersed in the fluid [4,5]. The effect is strongest in systems with long-range correlations, which give rise to long-range force. In many aspects, liquid-crystalline order can serve as a prime example of a correlated fluid, and the fluctuation-induced interaction in liquid crystals has already been studied in considerable extent [6–10].

The pioneering theoretical study in the field revealed a rich phenomenology of the effect in nematic, smectic, and columnar phases [6,7] as well as some of its most prominent consequences. Subsequently these results were extended to systems characterized by rugged substrates [8,9] and by finite strength of the surface interaction [10] and also to wetting geometries [11]. The common denominator of the liquid-crystalline and all other material counterparts of the Casimir effect is that the fluctuation-induced interaction is most important in uniformly ordered systems, which are, in fact, direct analogs of the electromagnetic vacuum as the ground state in the electrodynamic Casimir effect [1]. In uniform systems, the mean-field elastic energy and the corresponding interaction vanish, and the free energy of fluctuations is actually the lowest-order contribution to the total free energy.

Nowadays, microconfined liquid crystals are usually trapped in host materials with curved, irregular, or even fractal internal geometry [12], and one is tempted to believe that there are very few liquid-crystalline systems characterized by uniform director field. This notion relies on the reasoning that in systems with large surface-to-volume ratio the ordering is dictated by the surface interaction, implying that in microconfined geometries the equilibrium director field must be strongly distorted. But as pointed out in various contexts [13,14] this conclusion is often incorrect. This can be demonstrated by comparing the elastic energy associated with the distorted director field that satisfies the boundary conditions, which is inversely proportional to the thickness of the sample, and the (maximal) surface interaction energy, which does not depend on the thickness [14]. At thicknesses smaller than some critical value, the elastic free energy of the distorted structure would be larger than the maximal surface energy. In this case the equilibrium alignment is uniform and minimizes the elastic energy at the expense of the surface interaction.

This indicates that in microconfined liquid crystals uniform director configurations may not be that exotic at all. However, the director is not necessarily uniform throughout the sample: if the host geometry consists of a random system of small enough voids, the molecular arrangement within each void will be uniform but on a large scale the director field will be isotropic, resembling multidomain ordering in powder samples used in x-ray crystallography. On the other hand, local uniformity can also result in global order provided that the orientation of voids themselves is highly correlated.

Whatever the internal geometry of the host, the orientation of the director within a void is determined by the minimum of the surface energy. The molecular alignment is controlled by the strongest anchoring [15], whereas the effect of surface interaction in those parts of the internal surface where the boundary conditions are violated can be labeled as frustrating [16]—in the sense that it enhances fluctuations around the uniform configuration, and on increasing the characteristic distance d it eventually results in a structural transition to the distorted director structure [17].

It is quite natural to expect that the frustration-enhanced fluctuations give rise to a stronger pseudo-Casimir interaction compared to nonfrustrating geometries, and the aim of this paper is to analyze it theoretically in two model nematic systems that exemplify the physics of frustration. First, we focus on the hybrid-aligned film trapped between parallel substrates that enforce homeotropic and planar anchoring,

---

*Author to whom correspondence should be addressed. Electronic address: primoz.ziherl@ijs.si

respectively. In this geometry, which summarizes a number of features of microconfined systems, frustration arises from rival surface fields. Secondly, we examine the effect in the Fréedericksz cell where the liquid crystal is bounded by identical substrates and subjected to magnetic field which favors molecular orientation different from that imposed by the substrates. This is an example of competition between a surface field and a bulk field.

We limit the analysis to the long-range force induced by director modes. The interaction mediated by the degree of order, degree of biaxiality, and secondary director will be neglected: these components of the nematic order parameter are characterized by finite correlation lengths, and the corresponding force is short range both at the mean field [18] and fluctuational level [10]. We also disregard the substrate-stabilized presmectic ordering, which results in a short-range oscillatory mean-field force [19]. We restrict ourselves to the standard Frank Hamiltonian in the one-constant approximation and the Rapini-Papular surface interaction. Although this implies that some interesting phenomena—such as stripe domains associated with a finite saddle-splay elastic constant [20,21]—are put aside, the model still describes the pseudo-Casimir effect in frustrated geometries consistently.

We find that the effects of frustration can be very dramatic. Since it is rather difficult to avoid frustration at distances where the fluctuation-induced force is important, they are expected to control the force in most systems with characteristic size of the order of 10 nm. In particular, we show that the fluctuation-induced force in the hybrid cell is nonmonotonic, and that it is attractive at small distances and repulsive at distances comparable to the critical distance. This behavior represents a generalization of the existing theoretical understanding of the phenomenon in liquid crystals and in condensed matter in general. Moreover, at small distances the pseudo-Casimir force is the only source of structural interaction in the hybrid cell, and it is comparable in magnitude to the van der Waals force. This implies that the results reported actually cover a very important aspect of physics of a broad class of microconfined systems, since at distances of the order of 10 nm some external frustration is practically inevitable in any geometry.

We also analyze the fluctuation-induced force at the transition from uniform to distorted configuration, and we show that it diverges logarithmically at the critical thickness and that the divergence is universal. This suggests that the singularity—possibly truncated by the discontinuity of the transition—should also show up at structural transitions in curved and irregular geometries [12], which are characterized by topology-induced frustration.

The disposition of the paper is as follows. We begin with the fluctuation-induced interaction in the hybrid-aligned cell (Sec. II) and we turn to the Fréedericksz geometry in Sec. III. Along with the theoretical results, we also discuss the consequences of the effect as well as its observability. In Sec. IV we summarize the results and outline the main conclusions.

II. HYBRID-ALIGNED CELL

The main features of the substrate-induced frustration in confined liquid crystals can be modeled by the hybrid-
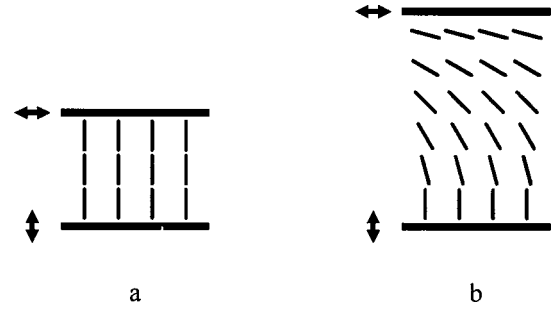

FIG. 1. The geometry of the homeotropic/planar hybrid cell. The homeotropic anchoring (bottom substrate) is assumed to be stronger than the planar anchoring (top substrate) so that in thin cells the director structure is homeotropic (a), whereas in thick cells it is distorted (b).

aligned nematic cell, which is of considerable technological importance for electrooptical applications in itself [22]. The cell consists of a nematic liquid crystal sandwiched between parallel but dissimilar substrates, the dissimilarity referring to the misalignment of the easy axes at the substrates. Dissimilar substrates usually differ in the anchoring strength as well, and the uniform director configuration is stable in thin hybrid cells with unlike anchoring strengths. Within the Rapini-Papular model of the surface free energy $F_{Si} = (K/2\lambda_i)\sin^2(\theta_i - \Theta_i)$ (where K is the effective elastic constant, λ_i is the extrapolation length at substrate i, and θ_i and Θ_i are the actual and the preferred polar angles of the director at substrate i), the uniform director structure is stable at thicknesses below the critical thickness $d_c = |\lambda_1 - \lambda_2|$, whereas for $d > d_c$ the director field is distorted [15,17,23].

To maximize the frustration, we assume that one plate favors homeotropic orientation of the director ($\Theta_1 = 0$) and that the other one is treated to induce degenerate planar anchoring ($\Theta_2 = \pi/2$) (Fig. 1). The model Hamiltonian consists of the one-constant Frank elastic energy and the Rapini-Papular surface interaction

$$H[\mathbf{n}] = \frac{K}{2}\left\{ \int [(\boldsymbol{\nabla}\cdot\mathbf{n})^2 + (\boldsymbol{\nabla}\times\mathbf{n})^2]\mathbf{d}V + \lambda_P^{-1} \right.$$
$$\left. \times \int (\mathbf{n}\cdot\mathbf{k})^2\mathbf{d}S_P - \lambda_H^{-1}\int (\mathbf{n}\cdot\mathbf{k})^2\mathbf{d}S_H\right\}, \quad (1)$$

where $\mathbf{n} = \mathbf{n}(\mathbf{r})$ is the nematic director, $\mathbf{k}$ is the normal of the plates, and λ_P and λ_H are the extrapolation lengths at the planar and homeotropic plate, respectively [24]. The surface terms are to be evaluated at the planar plate at $z = -d/2$ and at the homeotropic plate at $z = d/2$. We assume that the homeotropic anchoring is stronger than the planar anchoring (i.e., $\lambda_H < \lambda_P$) so that the uniform structure is homeotropic.

Within this model, the uniform structure is stable at thicknesses up to

$$d_c = \lambda_P - \lambda_H. \quad (2)$$

In the mean-field approximation, its free energy consists solely of the energetic penalty for an unfavorable director orientation at the planar plate

$$F_{\mathrm{MF}} = \frac{KS}{2\lambda_P}, \qquad (3)$$

where S is the cross section area of the cell. The mean-field free energy obviously does not depend on the thickness and hence does not induce any interaction between the plates, which implies that the interaction mediated by the fluctuations is the only source of the structural force.

A. Partition function

We analyze the fluctuations within the Gaussian approximation, which is expected to give a quantitatively correct description of the system at all d's except in the immediate vicinity of the transition which is continuous [17] and therefore associated with large fluctuations. Up to second order, the fluctuating director field can be written as

$$\mathbf{n} \approx (n_x, n_y, 1 - n_x^2/2 - n_y^2/2), \qquad (4)$$

and within the harmonic approximation the Hamiltonian is diagonal

$$H[n_x, n_y] = H[n_x] + H[n_y], \qquad (5)$$

where

$$H[n] = \frac{K}{2}\left[\int (\nabla n)^2 \mathbf{d}V - \lambda_P^{-1} \int n^2 \mathbf{d}S_P + \lambda_H^{-1} \int n^2 \mathbf{d}S_H \right]. \qquad (6)$$

The negative sign of the planar surface term is a clear signature of the frustrating role of the hybridity, which eventually destabilizes the uniform structure at $d = d_c$.

The two modes n_x and n_y are degenerate and we will consider just one of them. The free energy of fluctuations is determined by the partition function

$$\Xi = \exp(-F_{\mathrm{fluct}}/k_B T) = \int \mathcal{D}n \, \exp(-H[n]/k_B T), \qquad (7)$$

where n is either n_x or n_y, k_B is the Boltzmann constant, and T is the temperature. In any planar geometry, it is advantageous to make use of the in-plane translational invariance of the system and Fourier decompose the fluctuating fields, $n(\mathbf{r}) = \sum_{\mathbf{q}} \exp(i(q_x x + q_y y)) \tilde{n}(\mathbf{q}, z)$, where $\mathbf{q} = q_x \mathbf{i} + q_y \mathbf{j}$ and $\mathbf{i}$ and $\mathbf{j}$ are the in-plane components of the triad $(\mathbf{i}, \mathbf{j}, \mathbf{k})$ that spans the Cartesian coordinate system. This reduces $H[n]$ to an ensemble of harmonic oscillators

$$H[\tilde{n}] = \frac{KS}{2} \sum_{\mathbf{q}} \left[\int_{-d/2}^{d/2} (\tilde{n}'^2 + q^2\tilde{n}^2)\mathbf{d}z - \lambda_P^{-1}\tilde{n}_-^2 + \lambda_H^{-1}\tilde{n}_+^2 \right], \qquad (8)$$

where S is the area of the plates, prime stands for $\mathbf{d}/\mathbf{d}z$, and $\tilde{n}_\pm = \tilde{n}(z = \pm d/2)$. Now the partition function can be factorized, $\Xi = \Pi_{\mathbf{q}}\Xi_{\mathbf{q}}$, where $\Xi_{\mathbf{q}}$'s correspond to the partial Hamiltonians that make up $H[\tilde{n}]$, and the free energy of fluctuations can be written as

$$F_{\mathrm{fluct}} = -k_B T \sum_{\mathbf{q}} \ln \Xi_{\mathbf{q}}. \qquad (9)$$

Were there strong homeotropic anchoring conditions at the plates instead of homeotropic and planar anchoring of finite strength, the partial partition function $\Xi_{\mathbf{q}}$ would be equivalent to the propagator of a repelling quantum-mechanical harmonic oscillator that gives the probability for a particle in a repulsive parabolic potential to remain at a given point within a certain time interval. In this case, $\Xi_{\mathbf{q}} \propto [\sinh(qd)]^{-1/2}$ [25]. How can we generalize this result such as to allow for fluctuations at the plates? One way of doing this is based on the idea that a finite surface interaction with a given easy axis can be thought of as a superposition of strong surface interactions each characterized by some other easy axis and multiplied by the statistical weight corresponding to the energetic penalty for the deviation from the actual easy direction. In the language of quantum-mechanical propagators, such a procedure represents an extension of a point-to-point Green function to a region-to-region Green function, the width of each region being defined by a characteristic length analogous to the extrapolation length.

According to this recipe, the partition function is given by

$$\Xi_{\mathbf{q}} \propto \int_{-\infty}^{\infty} \mathbf{d}n_- \int_{-\infty}^{\infty} \mathbf{d}\tilde{n}_+$$
$$\times \exp\left(\frac{KS}{2k_B T}(\lambda_P^{-1}\tilde{n}_-^2 - \lambda_H^{-1}\tilde{n}_+^2) \right) \Xi_{\mathbf{q}; \tilde{n}_-, \tilde{n}_+}, \qquad (10)$$

where

$$\Xi_{\vec{q}; \tilde{n}_-, \tilde{n}_+} \propto \sqrt{\frac{1}{\sinh(qd)}} \exp\left(-\frac{KS}{2k_B T}q \right.$$
$$\left. \times \left[(\tilde{n}_-^2 + \tilde{n}_+^2)\coth(qd) - \frac{2\tilde{n}_-\tilde{n}_+}{\sinh(qd)} \right] \right) \qquad (11)$$

is the partition function associated with the boundary conditions $\tilde{n}(z = -d/2) = \tilde{n}_-$ and $\tilde{n}(z = d/2) = \tilde{n}_+$ [25]. After performing the elementary integrals in Eq. (10), we have

$$\Xi_{\mathbf{q}} \propto \left[\frac{q^2 - \lambda_P^{-1}\lambda_H^{-1}}{q(-\lambda_P^{-1} + \lambda_H^{-1})}\sinh(qd) + \cosh(qd) \right]^{-1/2}. \qquad (12)$$

This result [26] covers two known systems. For $\lambda_H = 0$ and $\lambda_P \to \infty$, i.e., strong homeotropic anchoring and infinitely weak planar anchoring, it reduces to the partition function corresponding to mixed, Dirichlet-Neumann boundary conditions [6,8]. Secondly, by setting $\lambda_H = -\lambda_P > 0$ one arrives at the partition function of fluctuations bounded by identical plates of finite anchoring strength [10].

Before focusing on the fluctuation-induced force, let us briefly discuss an interesting point related to the definition of the interaction free energy. In order to extract the interaction term from the total free energy, the partial partition function $\Xi_{\mathbf{q}}$ is usually rewritten as a product of three factors corresponding to bulk, surface, and interaction free energy. For example, in the case of strong anchoring at both plates, $\Xi_{\mathbf{q}} \propto [\sinh(qd)]^{-1/2}$, and $\sinh(qd)$ can be factorized to $\exp(qd) \times \frac{1}{2} \times [1 - \exp(-2qd)]$ [6]. This implies that the free energy of fluctuations with a given $\mathbf{q}$, $\ln \Xi_{\mathbf{q}}$, consists of a bulk term qd, which is proportional to d, a surface term $\ln(1/2)$, which
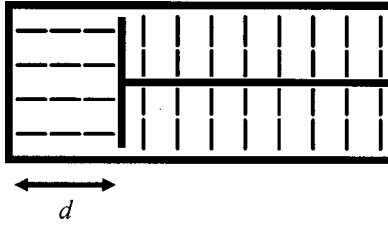
FIG. 2. A sketch of the gedanken experiment with the homeotropic director configuration in the confined section and the planar structure in the semi-infinite part of the setup.

is independent of d, and an interaction term $\ln(1-\exp(-2qd))$, which vanishes for $d\to\infty$. In the hybrid cell such a decomposition does not make much sense, because it leads to a surface term

$$\ln\left(\frac{(q+\lambda_H^{-1})(q-\lambda_P^{-1})}{q(-\lambda_P^{-1}+\lambda_H^{-1})}\right)$$

and an interaction term

$$\ln\left(1-\frac{q-\lambda_H^{-1}}{q+\lambda_H^{-1}}\frac{q+\lambda_P^{-1}}{q-\lambda_P^{-1}}\exp(-2qd)\right)$$

which do not exist at small q's although the underlying partition function itself is a well-defined quantity at all q's. In this case the factorization of

$$\frac{q^2-\lambda_P^{-1}\lambda_H^{-1}}{2q(-\lambda_P^{-1}+\lambda_H^{-1})}\sinh(qd)+\cosh(qd)$$

into components with the desired functional dependence on d does not result in three positive-definite factors but in one positive-definite and two either positive or negative factors. This does not bring about any conceptual dilemmas: it merely tells us that in the hybrid cell, surface and interaction free energy cannot be defined the same way as in the less complicated systems.

B. Fluctuation-induced force

The definition of the structural force

$$\mathcal{F}=-\left(\frac{\partial F}{\partial d}\right)_{S,V} \tag{13}$$

is most easily visualized by the cylinder-and-piston gedanken experiment (Fig. 2). The setup consists of a semi-infinite cylinder filled with a liquid crystal and equipped with a loose piston. If the piston is displaced from an initial position, the liquid crystal will flow either from or into the compartment between the piston and the end of the cylinder such that the volume and the surface of the system remain constant. The structural force is then defined as the force between the end of the cylinder and the piston, which implies that the interaction free energy is measured from the free energy of the reference bulk configuration.

To calculate the fluctuation-induced force, the single-oscillator partition function [Eq. (12)] is inserted into Eq. (9),

and the summation over $\mathbf{q}$'s is replaced by $(S/2\pi)\int_0^\infty qdq$. After subtracting the free energy of the bulk configuration and multiplying the force by 2 (there are 2 degenerate director modes), one is left with

$$\mathcal{F}_{\text{fluct}}=-\frac{k_BTS}{\pi}\int_0^\infty\frac{q^2dq}{\dfrac{q-\lambda_P^{-1}}{q+\lambda_P^{-1}}\dfrac{q+\lambda_H^{-1}}{q-\lambda_H^{-1}}\exp(2qd)-1}. \tag{14}$$

This integral cannot be computed analytically. However, one can work out the approximate behavior of the force in a couple of limiting regimes, and it is instructive to discuss them briefly before presenting numerical results. To keep the analytic approximations reasonably transparent, we restrict the discussion to strong anchoring at the homeotropic plate, i.e., $\lambda_H\to0$. In this case, $d_c=\lambda_P$. For small d/d_c's, which correspond to a weak destabilizing surface field at the planar plate, the fluctuation-induced force is given by

$$\mathcal{F}_{\text{fluct}}(\lambda_H/\lambda_P=0,d/d_c\ll1)\approx\frac{k_BTS}{2\pi}\left[\frac{3\zeta(3)}{8d^3}+\frac{\ln2}{\lambda_Pd^2}\right], \tag{15}$$

where $\zeta(3)=1.202\cdots$ is the Riemann zeta function $\zeta(s)=\sum_{m=1}^\infty m^{-s}$. The first term is nothing but the d^{-3} repulsion found in systems characterized by mixed (Dirichlet-Neumann) boundary conditions [6,8], which correspond to a cell bounded by a strong-anchoring plate and a zero-anchoring, inert plate. This is obviously the zeroth-order description of the hybrid cell in small d/d_c limit. The second term describes the effect of a weak but finite surface field at the planar plate, which promotes fluctuations and therefore enhances the discrepancy between the effective boundary conditions. This gives rise to an extra repulsion. The extra force is proportional to d^{-2} so that the larger the reduced distance, the more important the correction. Note that the magnitude of the correction is far from negligible: at $d/d_c=0.2$, the d^{-2} term represents as much as 25% of the total force.

One can also derive the dominant part of the fluctuation-induced force in the vicinity of the structural transition, where the destabilizing effect of the planar substrate is most prominent. For $\lambda_H/\lambda_P=0$ and $d/d_c\to1$, the force diverges logarithmically

$$\mathcal{F}_{\text{fluct}}(\lambda_H/\lambda_P=0,d/d_c\to1)\approx\frac{3k_BTS}{2\pi\lambda_P^3}\ln(3(1-d/d_c))^{-1}. \tag{16}$$

Although the singularity is not very strong, it definitely masks the basic d^{-3} repulsion. As we will see shortly, the repulsive singularity is a universal feature of pretransitional behavior of the fluctuation-induced interaction.

These analytical approximations fit very well with the numerical results for $\lambda_H\to0$ (Fig. 3). How does the force profile change if the homeotropic anchoring is not infinitely strong? As shown in Fig. 4, where the force is plotted versus the reduced distance for various relative strengths of the surface interactions, the fluctuation-induced force in a hybrid
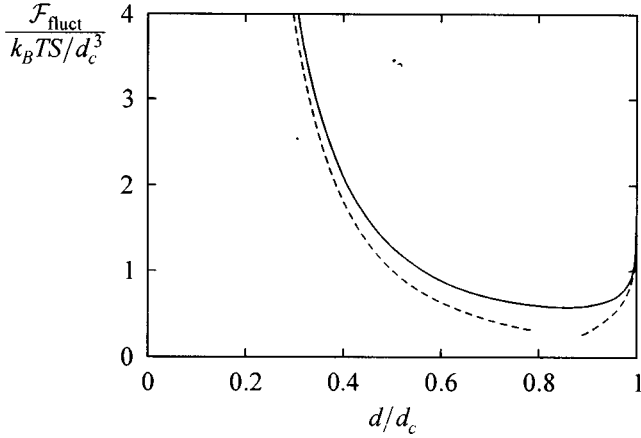
FIG. 3. Fluctuation-induced force in a hybrid cell with strong anchoring at the homeotropic plate: numerical result (solid line) and analytical approximations, Eqs. (15) and (16) (dashed lines). At the structural transition, the force diverges logarithmically.

FIG. 5. Crossover distance vs relative strength of the surface interactions. As long as the anchoring strengths are not too similar, d_0 increases approximately linearly with their ratio; at λ_H/λ_P larger than about 0.7, however, d_0 becomes virtually indistinguishable from d_c and the force is attractive at all distances except in the immediate vicinity of the critical thickness.

system with finite λ_H and λ_P departs significantly from the idealized model with $\lambda_H \to 0$. The generic force profile in real systems is as follows: the force is attractive at small d/d_c's, then it becomes repulsive, reaches a maximum, gradually fades out but levels off in the vicinity of the structural transition and eventually diverges at $d/d_c = 1$. If the anchoring strengths are not very different, the repulsive midrange maximum is absent and the small-d attractive regime extends almost right up to the structural transition. According to Fig. 5, the crossover distance which separates the attractive regime from the repulsive regime increases with λ_H/λ_P and so does the position of the maximal repulsion peak, which becomes progressively smaller and eventually vanishes for $\lambda_H/\lambda_P \gtrsim 0.26$. For λ_H/λ_P's larger than about 0.7, the crossover distance is virtually indistinguishable from

the critical thickness and the fluctuation-induced interaction is attractive almost right up to the transition.

At first sight, the transformation of the attractive force at small distances into a repulsive force at somewhat larger d/d_c's may seem a bit surprising. However, this kind of behavior is perfectly reasonable. At very small reduced thicknesses, both extrapolation lengths are larger than the thickness of the cell, which means that both planar and homeotropic surface interaction are effectively weak. In this limit, the fluctuations experience quasi-Neumann boundary conditions at both substrates so that the system is symmetric (Fig. 6), and in symmetric systems the fluctuation-induced force is attractive [6]. At thicknesses larger than the crossover distance, the homeotropic extrapolation length is smaller than the thickness of the cell—so that the anchoring at the homeotropic substrate is effectively strong—whereas the planar extrapolation length remains larger than d, which implies that the planar anchoring is still weak. In this case, the effective boundary conditions are mixed (quasi-Dirichlet at the homeotropic plate and quasi-Neumann at the planar plate) and in cells with mixed boundary conditions the interaction is known to be repulsive [6].

The second interesting feature of the fluctuation-induced interaction is its pretransitional divergence. According to Fig. 7, the singularity is logarithmic irrespective of the relative strength of anchorings, which is not unexpected because qualitatively the structural transition is the same for all λ_H/λ_P's. However, at the quantitative level these results may not describe the pretransitional behavior completely accurately because the harmonic model underestimates the magnitude of the fluctuations in the critical regime.

We have shown that the profile of the fluctuation-induced force in a hybrid geometry is nonmonotonic and fairly complex: attractive at small distances, repulsive at somewhat larger distances, and singular at the structural transition. This behavior is driven entirely by competing surface interactions, and is particularly important because the mean-field interaction is absent in thin hybrid cells. In many aspects, the geometry studied here can serve as a model of a number of
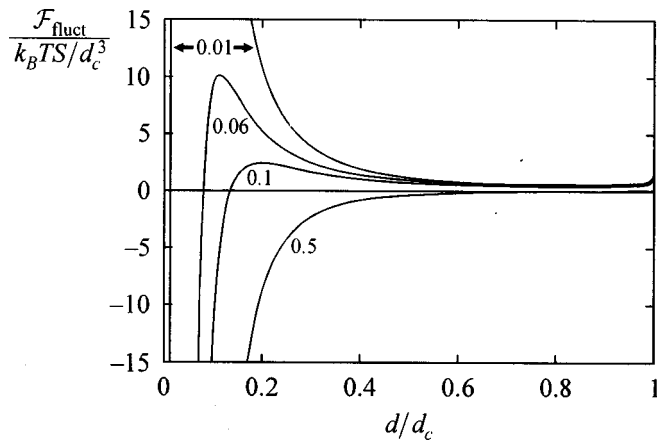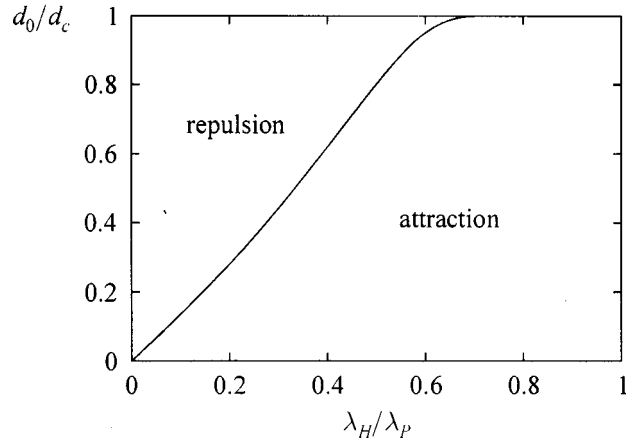

FIG. 4. Fluctuation-induced force in a hybrid cell with finite homeotropic anchoring versus the reduced distance for $\lambda_H/\lambda_P = 0.01, 0.0.06, 0.1$, and 0.5. At small distances the structural force is attractive, then it becomes repulsive, and at the transition it diverges. The crossover distance—where the attraction turns into repulsion—increases with the ratio of the extrapolation lengths, and for λ_H/λ_P's exceeding 0.26 the repulsive part of the force no longer reaches a maximum before the pretransitional singularity.
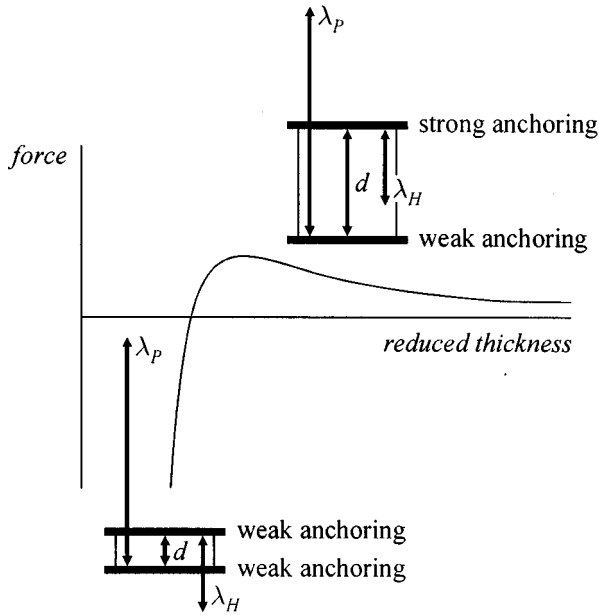
FIG. 6. A qualitative explanation of the mixed character of the structural force in the hybrid cell. At small thicknesses both extrapolation lengths are larger than d, which means that effective boundary conditions are weak (i.e., of Neumann-Neumann type) and interaction in symmetric systems is known to be attractive. At large d's the homeotropic anchoring becomes strong whereas the planar anchoring remains weak, and the fluctuations experience mixed, Dirichlet-Neumann boundary conditions, which result in repulsive interaction.

microconfined liquid-crystalline systems, the majority of which is characterized by frustration induced by the internal topology of the host medium.

C. Observability

How can the effect be detected? The crossed-cylinders arrangement usually used in surface force apparatus [27] is inappropriate because of curved geometry, and the classical experimental geometry based on a sandwich-type cell bounded by two glass plates is not suitable either because it
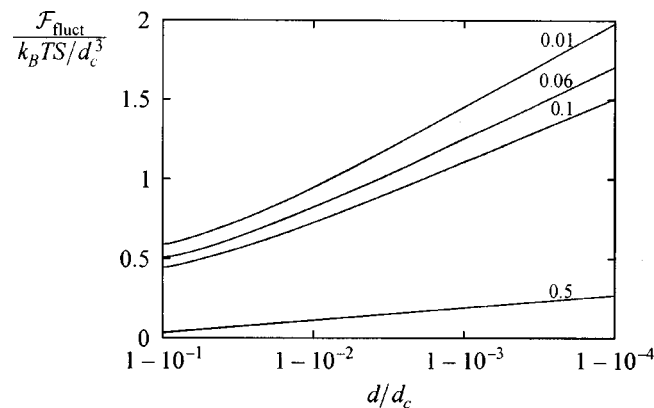

FIG. 7. A blow-up of Fig. 4 in the pretransitional regime. As stressed by this log-linear plot, the singularity is logarithmic regardless of the relative strength of the anchorings. As in Fig. 4, the curves are labeled by λ_H/λ_P.

is rather difficult to keep the substrates parallel at small distances. A truly planar sample can be prepared by spreading the liquid crystal on a substrate so that the upper surface of the film is free. At thicknesses such that $\partial \mathcal{F}_{\text{total}}/\partial d > 0$ (where $\mathcal{F}_{\text{total}}$ is the total force induced by the medium) such a film will disintegrate into an array of droplets and dry patches in a process called spinodal dewetting [28–30]. We have used the above results to reanalyze a recent experimental study of spinodal dewetting in 5CB [30] and we have shown that the fluctuation-induced interaction can provide a consistent and sound interpretation of the observed behavior [31]. This implies that the experiment in question [30] can be regarded as the first evidence of the pseudo-Casimir force in liquid crystals—a long sought-for support of theoretical efforts in the field.

Spinodal dewetting seems to be a well-suited tool for studies of structural forces for two reasons. First, the geometry of the film is well defined and simple, which facilitates the analysis, and secondly, there is no need for an external pressure gauge since the dewetting time and the size of the droplets are directly related to the structural force [28]. This means that one can actually map the force by continuously varying the initial thickness of the film and measuring the characteristic time and lengthscale of dewetting. However, dewetting occurs only for film thicknesses such that $\partial \mathcal{F}_{\text{total}}/\partial d > 0$, so that at some d's the structural force is not accessible. But this is quite common in force measurement techniques [32], and should not be considered a disadvantage specific for spinodal dewetting.

The structural interaction can be also studied by less direct methods. In fact, one could look for signatures of the interaction in liquid crystals confined to host media with irregular internal geometry. The size of voids in these systems is fixed and instead of measuring the force one should analyze finite-size effects in other experimental observables such as specific heat. There is a impressive quantity of unexplained or partly explained data on finite-size effects in liquid crystals [33–35] which may well depend on the phenomenon in question. But we will postpone the analysis of these data for a future study and extend the discussion of the fluctuation-induced interaction in frustrated systems from the hybrid cell to a system characterized by a bulk destabilizing force—the Fréedericksz cell.

III. FRÉEDERICKSZ CELL

Unlike the hybrid geometry, the Fréedericksz cell consists of identical substrates and the frustration is induced by magnetic field such that its easy direction is perpendicular to the molecular orientation preferred by the substrates. We first focus on the strong-anchoring limit which describes systems where the extrapolation length is much smaller than the critical thickness. In this case, the critical thickness for the transition from the uniform, substrate-aligned configuration to distorted, field-aligned configuration is given by

$$d_c = \pi \xi_M, \tag{17}$$

where

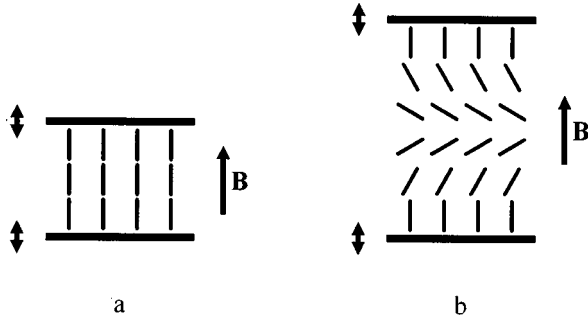$$\xi_M = \sqrt{\frac{\mu_0 K}{|\Delta \chi_a| B^2}} \tag{18}$$

FIG. 8. The Fréedericksz geometry: the low-field, substrate-aligned configuration (a) and the high-field, field-aligned configuration (b). The substrate-aligned configuration is homeotropic, and in a material with negative anisotropy of magnetic susceptibility the magnetic field normal to substrates favors planar orientation of the director.

is the magnetic coherence length; μ_0 is the magnetic permeability of vacuum, $\Delta\chi_a$ is the anisotropy of the magnetic susceptibility of the material, and B is the magnetic induction [24].

Let us first consider a liquid crystal with negative anisotropy of the magnetic susceptibility, e.g., 1-(trans-4-n-pentylcyclohexyl)-4'-cyanocyclohexane (CCH5). In such a case the magnetic torque tends to rotate the director towards the plane perpendicular to the magnetic field, and in order to destabilize the substrate-aligned configuration, **B** must be applied *along* the easy axis of the surface interaction (Fig. 8). In case of homeotropic anchoring, the Hamiltonian reads

$$H[\mathbf{n}] = \frac{K}{2} \int [(\mathbf{\nabla}\cdot\mathbf{n})^2 + (\mathbf{\nabla}\times\mathbf{n})^2 - \xi_M^{-2}(\mathbf{n}\cdot\mathbf{k})^2]\mathbf{d}V, \tag{19}$$

where **k** is the normal to the substrates. Strong anchoring requires that $\mathbf{n}(z = \pm d/2) = \mathbf{k}$.

The substrate-aligned configuration is identical as in the hybrid cell, and we will show that the systems are similar in several aspects. But there is a very important difference between them: in the hybrid cell, the mean-field interaction between the substrates is absent, whereas in the Fréedericksz cell the magnetic field generates a strong mean-field attraction. In the substrate-aligned state, the mean-field free energy consists of the magnetic energy

$$F_{MF} = \frac{KSd}{2\xi_M^2} \tag{20}$$

which is proportional to the volume of the cell. The corresponding thermodynamic force is obviously attractive and independent of thickness. As we will show, it is rather strong compared to the fluctuation-induced force. But before discussing the figures, let us analyze the fluctuation-induced interaction in detail.

A. Partition function

As in the hybrid cell, the two components of the fluctuating director field $\mathbf{n} \approx (n_x, n_y, 1 - n_x^2/2 - n_y^2/2)$ are degenerate. Their Hamiltonians are given by
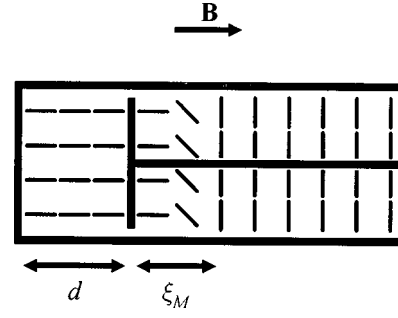

FIG. 9. The gedanken experiment with the Fréedericksz geometry. In the substrate-aligned configuration in the confined section of the setup, magnetic field destabilizes the director fluctuations, whereas in the field-aligned configuration (the semi-infinite compartment) it plays a stabilizing role. The nonuniform boundary layer in the semi-infinite part of the system is independent of d and does not contribute to the interaction free energy; its thickness is determined by the magnetic coherence length.

$$H[n] = \frac{K}{2} \int [(\nabla n)^2 - \xi_M^{-2} n^2]\mathbf{d}V, \tag{21}$$

where n is either n_x or n_y, and the boundary conditions read $n(z = \pm d/2) = 0$. After Fourier-transforming n and integrating the Hamiltonian over x and y, we obtain

$$H[\tilde{n}] = \frac{KS}{2} \sum_\mathbf{q} \int_{-d/2}^{d/2} [\tilde{n}'^2 + (q^2 - \xi_M^{-2})\tilde{n}^2]\mathbf{d}z. \tag{22}$$

The character of the partial Hamiltonians that make up $H[\tilde{n}]$ obviously depends on q: those with $q < \xi_M^{-1}$ correspond to attractive harmonic oscillators and those with $q > \xi_M^{-1}$ correspond to repelling harmonic oscillators [36]. In the first case, the partial partition function is proportional to $[\sin(q_< d)]^{-1/2}$, where $q_< = \sqrt{\xi_M^{-2} - q^2}$, and in the second case $\Xi_\mathbf{q} \propto [\sinh(q_> d)]^{-1/2}$, where $q_> = \sqrt{q^2 - \xi_M^{-2}}$.

This means that the free energy is given by

$$F_{fluct} = \frac{k_B T S}{2\pi} \left[\int_0^{\xi_M^{-1}} \ln\sin(q_< d)q_< \mathbf{d}q_< \right.$$
$$\left. + \int_0^\infty \ln\sinh(q_> d)q_> \mathbf{d}q_> \right]. \tag{23}$$

For d/ξ_M's larger than π—the Fréedericksz threshold—the first integral and therefore the whole partition function are undefined, because the transition is continuous.

The first integral in F_{fluct} is a pure interaction term, whereas the second one includes bulk, surface, and interaction free energy. To identify these terms properly, recall that the interaction free energy is measured from the free energy of the reference bulk configuration. In the hybrid cell, the bulk term of the Hamiltonian of the interplate region is identical to the Hamiltonian of the reference configuration, and the bulk free energy of the interplate region is identical to the free energy of the reference configuration. In the Fréedericksz cell, this is not the case: in the interplate region the magnetic field destabilizes the director fluctuations, whereas in the reference configuration it plays a stabilizing role (Fig. 9).

In the field-aligned state, the rotational symmetry of the system is broken. The director field is perpendicular to the magnetic field, and without loss of generality we can set **n** $\approx(1-n_y^2/2-n_z^2/2,n_y,n_z)$. The magnetic field does not affect director fluctuations parallel to **j**, but it does damp the fluctuations along **k**. The Hamiltonian reads

$$H_{\text{ref}}[n_y,n_z]=\frac{K}{2}\int[(\nabla n_y)^2+(\nabla n_z)^2+\xi_M^{-2}n_z^2]\mathbf{d}V \quad (24)$$

and the free energy of the reference bulk configuration is given by

$$\frac{k_BTSd}{4\pi}\left[\int_0^\infty q^2\mathbf{d}q+\int_{\xi_M^{-1}}^\infty q^2\mathbf{d}q\right], \quad (25)$$

where the first integral corresponds to the mode that is unaffected by the magnetic field (n_y) whereas the second one represents the free energy of the field-stabilized mode (n_z).

B. Fluctuation-induced force

Now the pseudo-Casimir force in the Fréedericksz cell can be calculated at once

$$\mathcal{F}_{\text{fluct}}=-\frac{k_BTS}{4\pi}\left[\frac{\zeta(3)}{d^3}+2\int_0^{\xi_M^{-1}}\cot(q_<d)q_<^2\mathbf{d}q_<+\frac{1}{3\xi_M^3}\right]. \quad (26)$$

The first term is the usual d^{-3} fluctuation-induced attraction in systems with long-range correlations [6], the second one describes an additional interaction caused by the destabilizing action of the magnetic field in the substrate-aligned configuration between the plates, and the third one is the constant attractive offset resulting from the difference between the bulk free energies of fluctuations in the substrate-aligned and the field-aligned configuration.

The functional behavior of the first and the last term is clear. What about the second one? For small reduced distances d/ξ_M,

$$\mathcal{F}_{\text{fluct}}(d/\xi_M\ll1)\approx-\frac{k_BTS}{4\pi}\left[\frac{\zeta(3)}{d^3}+\frac{1}{\xi_M^2d}\right]. \quad (27)$$

At small d/ξ_M's, the standard Casimir d^{-3} force obviously dominates, and the field-induced correction is proportional to d^{-1}.

If, on the other hand, the reduced distance d/ξ_M is close to the critical value π, the field-induced interaction can be approximated by

$$\mathcal{F}_{\text{fluct}}(d/\xi_M\to\pi)\approx\frac{k_BTS}{4\pi\xi_M^3}\left[\frac{2}{\pi}\ln(2\sin(d/\xi_M))^{-1}-\frac{1}{3}\right]. \quad (28)$$

In the vicinity of the threshold the fluctuation-induced force becomes repulsive and it diverges logarithmically—just as in the hybrid cell [Eq. (16)]. Although the systems are characterized by different destabilizing forces, they both undergo a similar transformation as the thickness is increased beyond
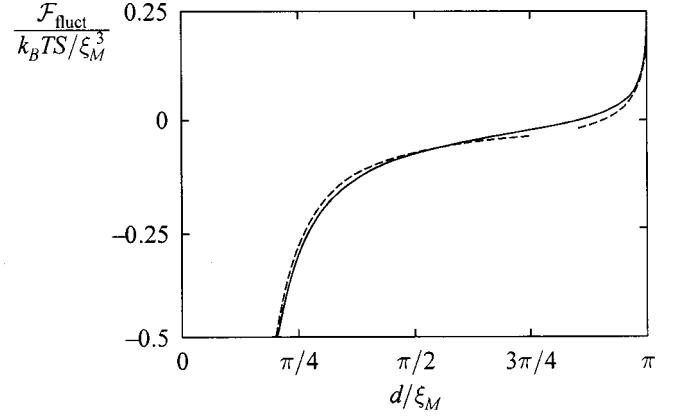

FIG. 10. Field-induced pseudo-Casimir force in nematic liquid crystals as a function of the reduced distance: at small distances the correction to the usual long-range d^{-3} attraction is proportional to d^{-1}, at $d/\xi_M=2.674$ the force becomes repulsive, and in the vicinity of the structural transition it diverges logarithmically just as in the hybrid cell. Solid line: exact result, dashed lines: analytical approximations.

the critical thickness. It is therefore not surprising that the pretransitional behavior of the fluctuation-induced force in the two systems is identical.

As in Sec. II, we find that the approximate formulas agree very well with the numerically calculated force (Fig. 10). As expected, the effect of the destabilizing magnetic field increases with the reduced distance, and the field-induced part of the interaction becomes comparable to the usual d^{-3} attraction found in nonfrustrated nematic liquid crystals at $d/\xi_M\simeq1.3$. The frustration caused by competing action of the magnetic field and the surface interaction controls the fluctuation-induced force in a wide range of thicknesses.

However, the structural interaction includes both fluctuation-induced and mean-field interaction [Eq. (20)] and the importance of the former can be quantified by the ratio of their magnitudes. We are interested primarily in the field-driven part of fluctuation-induced force: as implied by Eqs. (26) and (28), its magnitude scales as k_BTS/ξ_M^3. Apart from a numerical prefactor, the relative magnitude of the field-driven force is given by

$$\frac{k_BT}{K\xi_M}. \quad (29)$$

For $T=300$ K and $K=10^{-11}$ N, the force would become dominant for ξ_M's smaller than 0.4 nm. This implies that even in strongest magnets where the magnetic coherence length can be as short as 200 nm, the fluctuation-induced force amounts to a fraction of a percent of the mean-field force. Quite clearly, it will not be easy to measure an effect superposed to such a strong background. But the mean-field attraction is independent of thickness, and the pseudo-Casimir force could be detected by a setup sensitive to deviations from a constant background, which is, in fact, a situation encountered in many experimental studies.

C. Finite anchoring strength

A natural extension of this analysis is to loosen the surface interaction by replacing the strong anchoring boundary

conditions by a more realistic model. This is not expected to change any of the frustration-driven features of the pseudo-Casimir structural force significantly. However, at thicknesses where this force is important, the surface interaction cannot be described accurately by the strong anchoring approximation, and a brief discussion of the role of finite surface coupling may be helpful when analyzing or planning experiments.

We return to the field-destabilized Hamiltonian [Eq. (19)] and we substitute the strong-anchoring approximation by the homeotropic Rapini-Papoular surface terms. In this case

$$\mathcal{F}_{\text{fluct}} = -\frac{k_B T S}{\pi} \left[\int_0^\infty \frac{q^2 \mathbf{d}q}{\dfrac{(q+\lambda^{-1})^2}{(q-\lambda^{-1})^2} \exp(2qd) - 1} \right.$$
$$+ \frac{1}{2} \int_0^{\xi_M^{-1}} \frac{(\lambda^{-2} - q^2)\cot(qd) - 2q\lambda^{-1}}{(\lambda^{-2} - q^2) + 2q\lambda^{-1}\cot(qd)}$$
$$\left. \times q^2 \mathbf{d}q + \frac{1}{12\xi_M^3} \right]. \tag{30}$$

where λ is the extrapolation length. The first term, which describes the force in a weakly anchored nematic, has been already derived in a previous study [10]. The second term represents an extension of the field-destabilized part of the force and as long as the anchoring is rather strong (i.e., $\lambda < \xi_M$) it should not differ significantly from Eq. (26). The third term, which arises from the difference between bulk free energy densities in the substrate-aligned configuration and the reference field-aligned configuration, remains unaffected by λ.

The structure of the fluctuation-induced force implies that at least in the limit of strong but finite anchoring strengths, the finite-λ effect is simply superposed to the force driven by the destabilizing action of the magnetic field. This is shown in Fig. 11. We illustrate the roles of finite λ and ξ_M by plotting the ratio of the force at given λ and ξ_M and the usual long-range director attraction $-\zeta(3)k_B TS/4\pi d^3$, which represents the dominant part of the fluctuation-induced force at small distances. At distances comparable to the extrapolation length, the relative magnitude of the force is reduced, and the reduction is unaffected by the destabilizing effect of the magnetic field. On the other hand, the pretransitional behavior of the force is controlled by the magnetic field as long as λ is considerably smaller than ξ_M.

In the case of relatively weak anchoring the two effects are no longer separable. For $\lambda \sim \xi_M$, the anchoring-driven decrease of the magnitude of the force at $d \approx \lambda$ merges with the crossover from attraction to repulsion which occurs in the vicinity of the structural transition (Fig. 12). Secondly, in this regime the dependence of the critical thickness on the anchoring strength—described by the Rapini-Papoular equation [37]

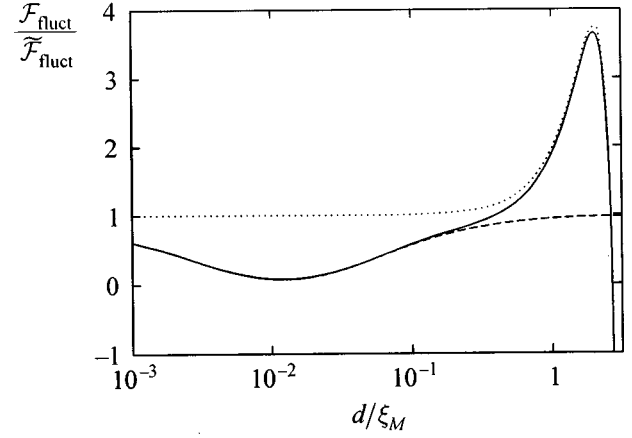$$d_c = 2\xi_M \text{arccot}(\lambda/\xi_M) \tag{31}$$

FIG. 11. The structure of the fluctuation-induced force in a weakly anchored Fréedericksz cell for $\lambda/\xi_M = 0.01$: shown here is the magnitude of the force relative to the usual long-range director attraction in symmetric systems $\tilde{\mathcal{F}}_{\text{fluct}} = -\zeta(3)k_B TS/4\pi d^3$ (solid line). As long as the extrapolation length is smaller than the magnetic coherence length, the anchoring-driven reduction of the force at distances comparable to λ is the same as in absence of the destabilizing magnetic field (dashed line), whereas the field-driven pretransitional behavior is virtually unaffected by anchoring and is described well by the strong-anchoring model (dotted line).

—becomes very prominent. However, the pretransitional repulsive singularity of the force remains logarithmic, which is, of course, expected.

D. Positive anisotropy of susceptibility

Let us now briefly address the phenomenon in materials with positive anisotropy of the magnetic susceptibility, where the Fréedericksz transition is induced by magnetic field applied perpendicular to the easy axis. The analysis of the fluctuation-induced interaction in this geometry is virtu-
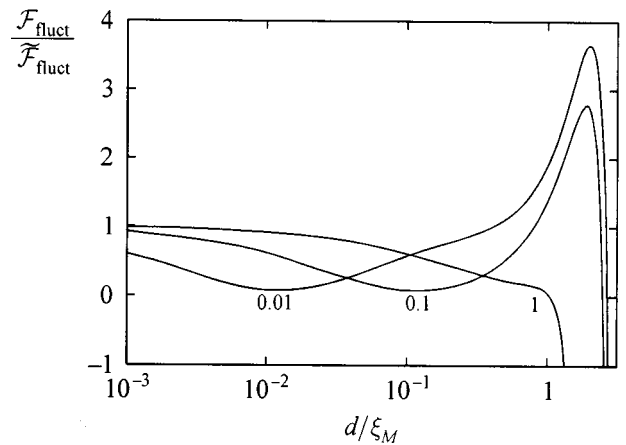

FIG. 12. Ratio of the fluctuation-induced force in a weakly anchored Fréedericksz cell for $\lambda/\xi_M = 0.01, 0.1$, and 1 and the usual long-range director attraction (see Fig. 11). If the extrapolation length is comparable to the magnetic coherence length, the interference of the effects of anchoring and the field-induced instability is no longer negligible. Note that the larger the extrapolation length, the smaller the critical thickness.

ally identical, the only difference being in the number of field-destabilized and field-stabilized modes in substrate-aligned and field-aligned configuration. If $\Delta\chi_a < 0$, the magnetic field destabilizes two director modes in the substrate-aligned configuration, and it stabilizes only one mode in the field-aligned configuration. On the other hand, if $\Delta\chi_a > 0$ it destabilizes only one mode in the substrate-aligned state and it stabilizes both modes in the field-aligned state. In the strong-anchoring limit, the pseudo-Casimir force in liquid crystals with $\Delta\chi_a > 0$ is given by

$$\mathcal{F}_{\text{fluct}} = -\frac{k_B T S}{4\pi}\left[\frac{\zeta(3)}{d^3} + \int_0^{\xi_M^{-1}}\cot(q_< d)q_<^2\,\mathbf{d}q_< + \frac{2}{3\xi_M^3}\right]. \tag{32}$$

Thus the magnitude of the constant fluctuation-induced attraction is twice as large as for $\Delta\chi_a < 0$, and the magnitude of the pretransitional divergence is twice smaller compared to systems with $\Delta\chi_a < 0$.

IV. CONCLUSIONS

In the study, we analyzed theoretically the fluctuation-induced interaction in two nematic cells characterized by competing external forces. We concentrated on the behavior of interaction at small distances where the director field is uniform rather than distorted. In the hybrid-aligned film the fluctuation-induced interaction is attractive at very small distances, whereas at distances comparable to but smaller than the critical distance it is repulsive. The force profile is non-monotonic except in cells with similar anchoring strengths. In the Fréedericksz cell, the fluctuation-induced force also exhibits a crossover from attraction at small distances to repulsion at large distances, but it is monotonic and mainly attractive.

The systems discussed are characterized by identical pretransitional behavior of the fluctuation-induced force. On approaching the transition from the uniform to the distorted director structure, the force becomes repulsive and it diverges at the critical thickness. We find that within the Gaussian approximation the singularity is logarithmic.

This indicates that the pretransitional behavior is universal. This is not difficult to understand once it has been realized that regardless of the source of the instability, every structural transition is induced by director fluctuations critically slowed down by an external force. The singularity must be intimately related to the soft mode that causes the instability. In the vicinity of the transition, the energy of this mode is proportional to $a(d_c - d) + (qd_c)^2$, where a is an appropriate constant. The free energy of fluctuations can be approximated by the contribution of the soft mode

$$F_{\text{fluct}} \approx \frac{k_B T S}{4\pi}\int_0^{q_{\max}}\ln(a(d_c - d) + (qd_c)^2)q\,\mathbf{d}q, \tag{33}$$

where we have introduced the short-wavelength cutoff $q_{\max}$ to make the discussion as transparent as possible. The value of the integral at the upper boundary, $q_{\max}$, does not really depend on d because $q_{\max}$ is very large (in the continuum limit $q_{\max}\rightarrow\infty$). This means that the structural force corresponding to a single soft mode is essentially given by

$$\mathcal{F}_{\text{fluct}} \approx \frac{k_B T S}{8\pi d_c^2}a\,\ln(a(d_c - d)), \tag{34}$$

which reproduces the functional form of the singularity found in the two model systems. As an illustration, let us apply this result to the Fréedericksz geometry, where the energy of the soft mode is proportional to $\pi^2[(d_c/d)^2 - 1] + (qd_c)^2$ and $d_c = \pi\xi_M$. In this case $a = 2\pi^2/d_c$, and after inserting it into Eq. (34) multiplied by 2—there are two soft modes in a cell with negative $\Delta\chi_a$— one reproduces the singular part of the force exactly.

Identical divergence is expected to occur in structural transitions in curved geometries, which can be considered driven by a generalized topological force. However, many transitions in curved geometries are accompanied by creation or annihilation of point defects, which makes them discontinuous. As a result, the singularity is shifted from a stable to a metastable state, which should lead to a truncated, cusplike force profile.

This is not the only generalization one can think of. External frustration, either field-driven or topology driven, is not inherent solely to the nematic phase and neither are the structural transitions it causes. In the more ordered liquid-crystalline phases the enhancement of the fluctuation-induced interaction due to competing external fields is undoubtedly marked by their structure, and it may well be quite different than in nematic phase. The analogs of the reported phenomena are not limited to liquid crystals, and the behavior of the fluctuation-induced force—the frustration-driven nonmonotonicity and the pretransitional singularity—is also important for the theory of the Casimir interaction in general [3]. The systems discussed illustrate that the phenomenology of the force can be rather complex even in relatively simple geometries, and that it can depart considerably from the types of force profiles known so far. It is possible that in other physical systems the effects of frustration are more striking and far reaching than in liquid crystals.

These results could help bridging the gap between theoretical and experimental efforts in the field. At distances where the fluctuation-induced force is relevant, the surface coupling should be modeled by finite interaction energy rather than by zero-parameter boundary conditions that give the simple power-law force profiles [6,7]. In this regime some frustration is present in any system, implying that the hybrid geometry describes a number of real systems—and that the observable fluctuation-induced force should in fact deviate from the ideal power-law behavior.

We have already used a part of this work to reanalyze the results of a recent experimental study of spinodal dewetting in a nematic liquid crystal [30], and we have shown that the observed dewetting of a thin film characterized by hybrid boundary conditions is driven by the fluctuation-induced force [31]. This means that the experiment in question provides the first evidence of the pseudo-Casimir effect in liquid crystals—and can be, along with experiments on binary liquid mixtures [38] and liquid helium [39], considered one of the pioneering experimental studies of the phenomenon in condensed matter.

Although the study is devoted primarily to theoretical aspects of the fluctuation-induced force, its findings may be

interesting from the technological point of view as well. With the development of electro-optical technology based on microconfined liquid crystals such as PDLC's [12], the characteristic lengthscale of the confinement has decreased considerably and it is expected that it will soon reach the range where the fluctuation-induced interaction is strong or even dominant. Since the *modus operandi* of most liquid-crystalline display devices relies on voltage-driven switching between two optically distinct director configurations, a de-tailed understanding of the structural interaction in liquid crystals in external field may be of considerable importance.

[1] H. B. G. Casimir, Proc. K. Ned. Akad. Wet. **51**, 793 (1948).

[2] H. B. G. Casimir and D. Polder, Phys. Rev. **73**, 360 (1948).

[3] S. Lamoreaux, Am. J. Phys. **67**, 850 (1999).

[4] M. Kardar and R. Golestanian, Rev. Mod. Phys. **71**, 1233 (1999).

[5] M. Krech, J. Phys. C **11**, R391 (1999).

[6] A. Ajdari, L. Peliti, and J. Prost, Phys. Rev. Lett. **66**, 1481 (1991).

[7] A. Ajdari, B. Duplantier, D. Hone, L. Peliti, and J. Prost, J. Phys. II **2**, 487 (1992).

[8] H. Li and M. Kardar, Phys. Rev. Lett. **67**, 3275 (1991).

[9] H. Li and M. Kardar, Phys. Rev. A **46**, 6490 (1992).

[10] P. Ziherl, R. Podgornik, and S. Žumer, Chem. Phys. Lett. **295**, 99 (1998).

[11] P. Ziherl, R. Podgornik, and S. Žumer, Phys. Rev. Lett. **82**, 1189 (1999).

[12] *Liquid Crystals in Complex Geometries*, edited by G. P. Crawford and S. Žumer (Taylor & Francis, London, 1996).

[13] J. B. Fournier and G. Durand, J. Phys. II **1**, 845 (1991).

[14] O. D. Lavrentovich, Liq. Cryst. **24**, 117 (1998), and references therein.

[15] A. Hochbaum and M. M. Labes, J. Appl. Phys. **82**, 2998 (1982).

[16] The frustration caused by the mismatch of the easy axes across the surface of the cavity or any other external forces is external and should not be mistaken for intrinsic frustration, which pertains to the intermolecular interaction and is also present in some liquid-crystalline systems [see, e.g., E. Fontes, P. A. Heiney, and W. H. de Jeu, Phys. Rev. Lett. **61**, 1202 (1988)].

[17] G. Barbero and R. Barberi, J. Phys. (Paris) **44**, 609 (1983).

[18] A. Poniewierski and T. J. Sluckin, Liq. Cryst. **2**, 281 (1987).

[19] P. G. de Gennes, Langmuir **6**, 1448 (1990).

[20] O. D. Lavrentovich and V. M. Pergamenshchik, Mol. Cryst. Liq. Cryst. **179**, 125 (1990).

[21] V. M. Pergamenshchik, Phys. Rev. E **47**, 1881 (1993).

[22] S. Matsumoto, M. Kawamoto, and K. Mizunoya, J. Appl. Phys. **47**, 3842 (1976).

[23] The transition from uniform to distorted structure is direct only within the director description of nematic order. In the Landau–de Gennes theory, the two structures are separated by the biaxial structure characterized by uniform director field and nonuniform profiles of the degrees of order and biaxiality—the so-called eigenvalue exchange configuration [P. Palffy-Muhoray, E. C. Gartland, and J. R. Kelly, Liq. Cryst. **16**, 713 (1994); A. Šarlah and S. Žumer, Phys. Rev. E **60**, 1821 (1999)]. However, deep in the nematic phase the biaxial structure is stable in a very narrow range of thicknesses so that it can be neglected without compromising the basic physics of the hybrid cell.

[24] P. G. de Gennes and J. Prost, *The Physics of Liquid Crystals* (Clarendon, Oxford, 1993).

[25] H. Kleinert, *Path Integrals in Quantum Mechanics, Statistics, and Polymer Physics* (World Scientific, Singapore, 1995).

[26] Note that $\Xi_{\mathbf{q}}$ does not exist for arbitrary values of d, λ_P, and λ_H, because $(q^2 - \lambda_P^{-1}\lambda_H^{-1})/q(-\lambda_P^{-1} + \lambda_H^{-1})\sinh(qd) + \cosh(qd)$ (the inverse square of $\Xi_{\mathbf{q}}$) can be negative at small q's. Up to second order in q, this expression is given by $(1 - d/d_c) + d/d_c(\lambda_P\lambda_H/d_c^2 + d/2d_c - d^2/6d_c^2)(qd_c)^2$, which becomes negative for d's larger than d_c. The partition function of fluctuations is undefined beyond the structural transition—which is continuous.

[27] J. N. Israelachvili, *Intermolecular and Surface Forces* (Academic, London, 1992).

[28] F. Brochard Wyart and J. Daillant, Can. J. Phys. **68**, 1084 (1989).

[29] S. Herminghaus, K. Jacobs, K. Mecke, J. Bischof, A. Fery, M. Ibn-Elhaj, and S. Schlagowski, Science **282**, 916 (1998).

[30] F. Vandenbrouck, M. P. Valignat, and A. M. Cazabat, Phys. Rev. Lett. **82**, 2693 (1999).

[31] P. Ziherl, R. Podgornik, and S. Žumer, Phys. Rev. Lett. **84**, 1228 (2000).

[32] J. N. Israelachvili and G. E. Adams, J. Chem. Soc. Faraday Trans. I **74**, 975 (1978).

[33] G. S. Iannacchione, G. P. Crawford, S. Qian, J. W. Doane, D. Finotello, and S. Žumer, Phys. Rev. E **53**, 2402 (1996).

[34] H. Haga and C. W. Garland, Phys. Rev. E **56**, 3044 (1997).

[35] G. S. Iannacchione, C. W. Garland, J. T. Mang, and T. P. Rieker, Phys. Rev. E **58**, 5966 (1998).

[36] C. Grosche and F. Steiner, *Handbook of Path Integrals* (Springer Verlag, Berlin, 1998).

[37] A. Rapini and M. Papoular, J. Phys. Colloq. **30**, C4-54 (1969).

[38] A. Mukhopadhyay and B. M. Law, Phys. Rev. Lett. **83**, 772 (1999).

[39] R. Garcia and M. H. W. Chan, Phys. Rev. Lett. **83**, 1187 (1999).